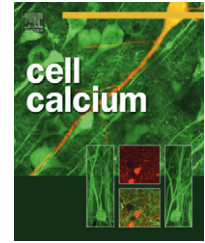




ELSEVIER

journal homepage: www.elsevier.com/locate/ceca



Local induction of pacemaking activity in a monolayer of electrically coupled quiescent NRK fibroblasts

M.M. Dernison^{a,1}, J.M.A.M. Kusters^{b,1}, P.H.J. Peters^a,
W.P.M. van Meerwijk^a, D.L. Ypey^a, C.C.A.M. Gielen^b,
E.J.J. van Zoelen^a, A.P.R. Theuvenet^{a,*}

^a Department of Cell Biology, Radboud University Nijmegen, Heyendaalseweg 135, 6526 AJ Nijmegen, The Netherlands

^b Department of Biophysics, Radboud University Nijmegen, Geert Groteplein 21, 6525 EZ Nijmegen, The Netherlands

Received 19 October 2007; received in revised form 22 December 2007; accepted 11 February 2008

Available online 24 March 2008

KEYWORDS

IP₃;
L-type calcium channel;
Synchronization;
Calcium action potential;
PGF_{2α}

Summary Cultures of normal rat kidney (NRK) fibroblasts may display spontaneous calcium action potentials which propagate throughout the cellular monolayer. Pacemaking activity of NRK cells was studied by patch clamp electrophysiology and vital calcium imaging, using a new experimental approach in which a ring was placed on the monolayer in order to physically separate pacemakers within or under the ring and follower cells outside the ring. Stimulation of cells inside the ring with IP₃-generating hormones such as prostaglandin F_{2α} (PGF_{2α}) resulted in the induction of periodic action potentials outside the ring, which were abolished when the L-type calcium channel blocker nifedipine was added outside the ring, but not inside the ring. PGF_{2α}-treated cells displayed asynchronous IP₃-mediated calcium oscillations of variable frequency, while follower cells outside the ring showed synchronous calcium transients which coincided with the propagating action potential. Mathematical modelling indicated that addition of PGF_{2α} inside the ring induced both a membrane potential gradient and an intracellular IP₃ gradient, both of which are essential for the induction of pacemaking activity under the ring. These data show that intercellular coupling between PGF_{2α}-treated and non-treated cells is essential for the generation of a functional pacemaker area whereby synchronization of calcium oscillations occurs by activation of L-type calcium channels.

© 2008 Elsevier Ltd. All rights reserved.

Introduction

Spontaneous calcium action potentials have been identified in a variety of tissues, from smooth muscle, endocrine and neuronal origin [1–3]. We have shown before that density-arrested monolayers of normal rat kidney (NRK) fibroblasts in

* Corresponding author. Tel.: +31 24 3652013; fax: +31 24 3652999.

E-mail address: a.theuvenet@science.ru.nl (A.P.R. Theuvenet).

¹ These authors have contributed equally.

tissue culture display propagating calcium action potentials [4–7]. Such propagating action potentials generally require a combination of so-called pacemaker and follower cells. In the smooth muscle layers of the gastrointestinal and urinary tract, as well as of the fallopian tubes, the interstitial cells of Cajal (ICC) or ICC-like cells have been shown to function as pacemakers which induce propagating calcium action potentials in their surrounding follower cells [1,8–12]. Recently evidence was found for ICC-like cells associated with vascular smooth muscle layer, although their role in vasomotion remains elusive [13]. However, NRK fibroblasts have been derived from a single clone and are therefore genetically homogeneous. As a consequence specific molecular markers for identification of pacemaking cells in such cultures are lacking, which makes it difficult to identify pacemaking cells and to study the mechanisms involved in the generation of action potentials.

NRK fibroblasts form an attractive model system to study action potential generation, since their initiation and propagation is related to the growth status of the cells [6]. Confluent cells made quiescent by serum deprivation are electrically coupled, have a membrane potential of -70 mV, but do not spontaneously fire calcium action potentials. However, local addition of a depolarizing agent such as K^+ to these cells results in the induction of a single calcium action potential, which propagates throughout the monolayer [4]. This observation indicates that quiescent NRK cells have all the properties of follower cells, but the cultures appear to lack cells with pacemaking activity. Upon addition of epidermal growth factor (EGF) and insulin, quiescent cells grow to density-arrest within 48 h. Such density-arrested cells have a membrane potential of -70 mV, and show periodic propagating calcium action potentials during which the membrane depolarizes to positive values [5]. Upon subsequent addition of retinoic acid or transforming growth factor- β , these density-arrested cells are restimulated to proliferate and undergo phenotypic transformation after 48 h, resulting in a constitutively depolarized membrane potential of -20 mV in the absence of action potentials [6].

Prostaglandin $F_{2\alpha}$ ($PGF_{2\alpha}$) plays an important role in the different growth states of NRK fibroblasts. Addition of $PGF_{2\alpha}$ to quiescent or density-arrested monolayers of NRK fibroblasts results in the generation of asynchronous IP_3 -mediated calcium oscillations associated with a sustained depolarization to -20 mV [14]. Furthermore, phenotypically transformed NRK cells show autocrine production of $PGF_{2\alpha}$ which is responsible for the observed depolarization, since phenotypically transformed NRK cells in which the expression of the $PGF_{2\alpha}$ receptor (Ptgfr) is knocked down by an shRNA approach, have a membrane potential of -70 mV (W.H. Almirza, unpublished observations). Removal of secreted $PGF_{2\alpha}$ by perfusion of transformed NRK cells with fresh medium resulted in a repolarization accompanied by the spontaneous generation of action potentials [6]. The observation of spontaneous action potentials in density-arrested monolayers, indicates that both pacemaker and follower cells must be present in these cultures. We have proposed that density-arrested cells with their membrane potential of -70 mV basically behave as follower cells, but that groups of cells within the monolayer are able to secrete enhanced levels of $PGF_{2\alpha}$, and that groups of cells within the monolayer are able to secrete enhanced levels of $PGF_{2\alpha}$,

and thereby induce pacemaking activity. In earlier studies it has been shown that L-type calcium channels are essential for the propagation of calcium action potentials in NRK monolayers, since action potential propagation is inhibited by nifedipine and other blockers of L-type calcium channels [4,5].

In the present study we analyzed the properties of NRK pacemaker and follower cells in detail, by making an experimental set-up in which both cell types were physically separated. This was achieved by applying a cloning ring on top of a confluent monolayer of quiescent NRK cells, whereby the addition of $PGF_{2\alpha}$ to the cells inside the ring evoked pacemaking activity, while the perfused cells outside the ring behaved as follower cells. Using this approach we show by a combination of experimental and modeling studies that both the $PGF_{2\alpha}$ -treated cells and the follower cells are required for the generation of zonal pacemaker areas, which are located in areas just outside the regions with $PGF_{2\alpha}$ -treated cells. In the present experimental set-up those pacemaker areas are formed under the ring. A $PGF_{2\alpha}$ -induced membrane potential gradient is established just outside the inner diameter of the ring, in combination with an intracellular IP_3 -concentration gradient. In contrast to results of previous studies [15,16] pacemaking activity in NRK monolayers does not seem to require intercellular diffusion of Ca^{2+} .

Materials and methods

Cell culturing: Normal rat kidney fibroblasts (NRK clone 49F) were cultured in bicarbonate-buffered Dulbecco's modified Eagle's medium (DMEM; Invitrogen, Paisley, UK) supplemented with 10% newborn calf serum (HyClone Laboratories, Logan, UT, USA). For electrophysiology experiments, 1.0×10^5 NRK cells were seeded in 8.8 cm² dishes. For calcium imaging experiments 1.2×10^5 NRK cells were seeded on 0.1% gelatin-coated glass coverslips with a diameter of 25 mm in 9.6 cm² wells. In both cultures cells reached confluency after four days. Cells were then incubated for three days in serum-free DF medium (1:1 mixture of DMEM and Ham's F-12 medium; Invitrogen, Paisley, UK) supplemented with 30 nM Na_2SeO_3 and 10 μ g/ml human transferrin, to obtain quiescent cells. Prior to electrophysiological and calcium imaging measurements, a small cloning ring of acrylic glass was placed on top of the monolayer without disrupting intercellular contact, thereby isolating the medium inside the ring (approximately 70 μ l of serum-free DF-medium in the electrophysiological and 40 μ l of calcium containing HEPES-buffered saline in the calcium imaging measurements) from the perfused medium outside the ring. The outside diameter of the ring was 8 mm and the inside diameter 6 mm (height 8 mm), thereby enclosing approximately 3.0×10^4 cells within the ring. Endothelin-1 and $PGF_{2\alpha}$ were purchased from Sigma (St. Louis, MO, USA), bradykinin was purchased from Boehringer (Mannheim, Germany).

Electrophysiology: Whole cell current clamp experiments on quiescent NRK fibroblasts were performed at room temperature as described previously [6]. At the start of the recordings cells were perfused with serum-free DF medium equilibrated with 7.5% CO_2 , pH 7.4. After approximately 5 min this medium was replaced by Sr^{2+} -containing HEPES-

buffered saline (Sr^{2+} -HBS) containing 135.5 mM NaCl, 5.0 mM KCl, 5.0 mM SrCl_2 , 1.0 mM MgCl_2 , 10 mM glucose and 10 mM HEPES-KOH, pH 7.4. Sr^{2+} was used instead of Ca^{2+} to enhance generation and propagation of action potentials in the cultures upon addition of $\text{PGF}_{2\alpha}$ [5]. Action potentials were measured outside the ring using borosilicate patch pipettes (GC150-15; Clark, Reading, UK) with resistances of 4–6 M Ω , with an intracellular pipette solution containing 25 mM NaCl, 120 mM KCl, 1.0 mM CaCl_2 , 1.0 mM MgCl_2 , 3.5 mM EGTA, and 10 mM HEPES-KOH, pH 7.4. Data were acquired with an HEKA EPC-10 patch-clamp amplifier in conjunction with Pulse/Pulsefit v8.74 software (HEKA Elektronik, Lambrecht, Germany) at a sampling frequency of 0.1 kHz. Data analysis was performed offline using Microcal Origin software version 6.0 (Microcal Software, Northampton, MA, USA).

Intracellular calcium measurements: Glass coverslips containing quiescent monolayers of NRK fibroblasts were placed in a Leiden cell chamber and loaded for 30 min with 4 μM Fura-2/AM (Invitrogen, Eugene, OR, USA) in serum-free DF medium at room temperature. Prior to the placement of the ring, the loading medium was replaced by Ca^{2+} containing HEPES-buffered saline (Ca^{2+} -HBS, containing 141.5 mM NaCl, 5.0 mM KCl, 1.0 mM CaCl_2 , 1.0 mM MgCl_2 , 10 mM glucose, 10 mM HEPES-KOH, pH 7.4). Before starting the recordings the medium outside the ring was perfused with Sr^{2+} -HBS. Inside the ring the Ca^{2+} -HBS was not replaced by Sr^{2+} -HBS because the lower affinity of Fura-2 for Sr^{2+} than for Ca^{2+} might obscure the detection of the changes in Fura-2 fluorescence ratios due to the rather small IP_3 -induced releases of Ca^{2+} from the intracellular calcium stores. Dynamic calcium video imaging, both inside, outside and under the ring, was performed as described elsewhere [17]. Excitation wavelengths of 340 and 380 nm (bandwidth 8–15 nm) were provided by a 150 W Xenon lamp (Ushio UXL S150 MO, Ushio, Tokyo, Japan), while fluorescence emission was monitored above 440 nm, using a 440 nm DCLP dichroic mirror in front of the camera. Image acquisition, using a camera pixel binning of 4 and computation of ratio images (F340/F380), was every 4 s and operated through Metafluor v.6.2 (Universal Imaging Corporation, Downingtown, PA, USA). Camera acquisition time was 100 ms per excitation wavelength. Oscillations in intracellular Ca^{2+} -concentration were analyzed by a custom made analysis protocol in Wolfram Mathematica version 6, in order to determine the time points at which the peak of a Ca^{2+} -wave occurred, as well as the time interval between the subsequent peaks (interval time). The bin size of the histograms of interval time was 5 s.

Mathematical modeling: Computer simulations were performed using the mathematical model of normal rat kidney (NRK) fibroblasts reported in previous studies [18–20]. Each cell in the model consists of two compartments: a single calcium store, located in the endoplasmic reticulum (ER), and the cytosol. The plasma membrane of each cell contains gap junctions to neighboring cells, calcium-activated chloride-channels, L-type calcium-channels ($\text{CaV} 1.2$), Ca^{2+} -ATPase (PMCA), inward-rectifier potassium-channels, store-dependent calcium-channels and a passive leak. The ER membrane contains IP_3 -receptors, Ca^{2+} -ATPase (SERCA) and a passive leak. The characteristics of the various ion channels have previously been determined for NRK cells

using single-cell measurements [14]. In the model each cell has a fixed intracellular IP_3 -concentration, which thereby affects calcium oscillations by regulating the speed of inactivation of the IP_3 -receptor [19,21].

The model describes the dynamics of the membrane potential, the transmembrane currents and the intracellular calcium oscillator, based on a coupling between the kinetics of the excitable membrane and that of the intracellular calcium oscillator by cytosolic calcium [19]. Moreover, the model explains the generation and propagation of repetitive action potentials and calcium waves in a one-dimensional network of NRK cells [20]. Details of the model and the parameter values used in the simulations have been presented previously [19,20]. According to the model, the local addition of hormones such as $\text{PGF}_{2\alpha}$ will generate IP_3 -mediated intracellular Ca^{2+} -oscillations in their target cells. The enhanced Ca^{2+} -concentration results in opening of the calcium-activated chloride-channels, resulting in a depolarization of the cell towards the chloride Nernst potential near -20 mV and subsequent activation of the L-type calcium-channels. Opening of these calcium channels will generate an influx of Ca^{2+} into the cells, resulting in a rapid but transient depolarization towards the positive equilibrium potential for calcium ions. The calcium-activated chloride-channels will remain activated as long as the intracellular Ca^{2+} -concentration is elevated, resulting in a plateau phase at the chloride Nernst potential at -20 mV. Upon extrusion of Ca^{2+} from the cytoplasm by calcium ATPases, the calcium-activated chloride-channels become deactivated, and the cells will subsequently repolarize to -70 mV as a result of the activity of inward-rectifier K^+ -channels [7]. Transmission of the action potential to the follower cells requires depolarization of neighboring cells through gap junctions, which results in opening of their L-type calcium channels and the firing of an action potential.

In the present study we use a two-dimensional layer of cells with the above properties to analyze our experimental findings. The cells are coupled to their nearest neighbors in a hexagonal grid by gap junctions. Gap junctions provide not only the intercellular diffusion pathway for IP_3 but an electrical coupling of the cells as well. The mathematical coupling between cells in this model occurs by electrical current through the gap junctions with an intercellular conductance of 3 nS, which is driven by the membrane potential difference between the cells.

For our modeling we used a hexagonal grid consisting of cells with a diameter of 10 μm . The complete network included 400 \times 400 cells. In the simulations a ring with an outer diameter of 3 mm and an inner diameter of 2 mm was used, resulting in a circular two-dimensional cluster of NRK cells. A ring with a diameter smaller than that used in the experiments (6–8 mm) was chosen, in order to reduce the computing time of the computer simulations of the network. The 31,000 cells inside the ring were given a fixed IP_3 -concentration for each cell, randomly chosen between 5 and 15 μM , to mimic the differences in the frequency of intracellular Ca^{2+} -oscillations experimentally observed for various cells [14]. The cells far outside the ring were set at an IP_3 -concentration of 0.1 μM . In the transitional zone between these groups of cells IP_3 was distributed according to a radial gradient as a result of diffusion of IP_3 , as described in Appendix A.

Results

Agonists of G-protein coupled receptors induce pacemaking activity

Density-arrested NRK monolayers display spontaneous calcium action potentials and are therefore supposed to contain both pacemaker and follower cells. To study under which conditions pacemaking activity can be generated and action potentials are initiated, we placed a 6–8 mm ring on top of a confluent monolayer of quiescent NRK cells, which separates the medium inside the ring from the perfused medium outside the ring, without perturbing the gap junction-mediated intercellular communication between these cells. This approach allowed us to study the propagation of calcium action potentials outside the ring, as a result of the addition of hormonal triggers inside the ring. Membrane potential recordings were performed only outside the ring (5–10 mm from the ring), while calcium imaging measurements were performed outside (5–10 mm from the ring), inside and under the ring.

Fig. 1A shows that addition of $0.5 \mu\text{M}$ $\text{PGF}_{2\alpha}$ inside the ring can induce periodic action potentials in cells outside the ring. Such action potentials were observed in 19 out of 24 experiments, and were initiated within 10 min after addition of $\text{PGF}_{2\alpha}$ (median time 4.5 min). In 11 of 13 calcium imaging recordings synchronous calcium waves were observed within 10 min after addition of $\text{PGF}_{2\alpha}$ (median value 3.8 min, Fig. 2). The mean interval time between successive action potentials was 3.5 ± 0.6 min (mean \pm S.E.M.; $n=19$). Similar results were obtained with other activators of Gq-coupled receptors, including endothelin-1 ($n=3$) and bradykinin ($n=2$). However, addition of 30 mM K^+ inside the ring, which induced a similar depolarization of the cells as $\text{PGF}_{2\alpha}$ (-20 mV), generated either no ($n=5$) or typically only one single propagating action potential in cells outside the ring ($n=3$). The observation that $\text{PGF}_{2\alpha}$ induced repetitive action potentials, while K^+ induced at most a single action potential, suggests that the induction of periodic calcium action potentials requires not only depolarization of cells inside the ring, but also the sustained production of intracellular second messengers such as IP_3 from activated Gq-coupled receptors.

Blocking of L-type calcium channels in $\text{PGF}_{2\alpha}$ -treated cells does not inhibit pacemaking activity

Activation of L-type calcium channels is essential for the generation and propagation of calcium action potentials [4,5]. The ring approach allowed us to study the effect of inhibition of L-type calcium channels separately on hormone-treated cells and follower cells. Fig. 1B shows that addition of $0.3 \mu\text{M}$ nifedipine inside the ring does not impair $\text{PGF}_{2\alpha}$ -induced generation and propagation of calcium action potentials outside the ring ($n=4$). However, subsequent addition of nifedipine outside the ring resulted in the immediate inhibition of firing of these action potentials ($n=4$). $\text{PGF}_{2\alpha}$ -induced calcium oscillations of cells inside the ring were not affected upon exposure of these cells to nifedipine

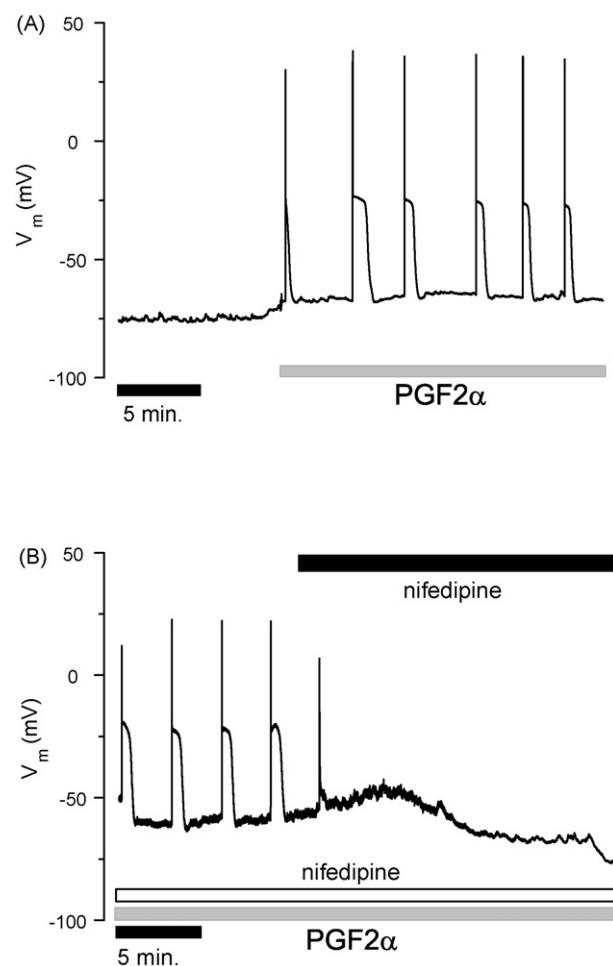


Figure 1 Action potentials recorded outside the ring are induced by $\text{PGF}_{2\alpha}$ inside the ring and inhibited by addition of nifedipine outside the ring. (A) Typical membrane potential response of NRK fibroblasts ($n=24$) measured outside the ring after addition of $0.5 \mu\text{M}$ $\text{PGF}_{2\alpha}$ inside the ring (indicated by lower light gray bar). (B) Typical membrane potential response ($n=4$) measured outside the ring after addition of $0.3 \mu\text{M}$ nifedipine inside the ring (indicated by lower open bar), and following perfusion with $0.3 \mu\text{M}$ nifedipine outside the ring (indicated by upper dark gray bar). Trace in (B) is preceded by the trace presented in (A). In all figures additions inside the ring are indicated by lower bars, additions outside the ring are indicated by the upper bars. Time (5 min) is indicated by the lower black bar.

(see Supplemental file 1), in accordance with previous findings that perfusion of a whole monolayer with nifedipine did not affect the asynchronous $\text{PGF}_{2\alpha}$ -induced calcium oscillations in the NRK fibroblasts [14]. These data agree with previous observations that in $\text{PGF}_{2\alpha}$ -treated cells the L-type calcium channels are inactivated due to auto-inhibition by Ca^{2+} and voltage-dependent inactivation [5,22]. Therefore, blocking these channels by adding nifedipine does not annihilate the pacemaking mechanism evoked by $\text{PGF}_{2\alpha}$ -addition in the ring. From this experiment we conclude that the $\text{PGF}_{2\alpha}$ -treated cells are essential for pacemaking activity but are themselves not the actual pacemaker cells which set the frequency of follower cells outside the ring.

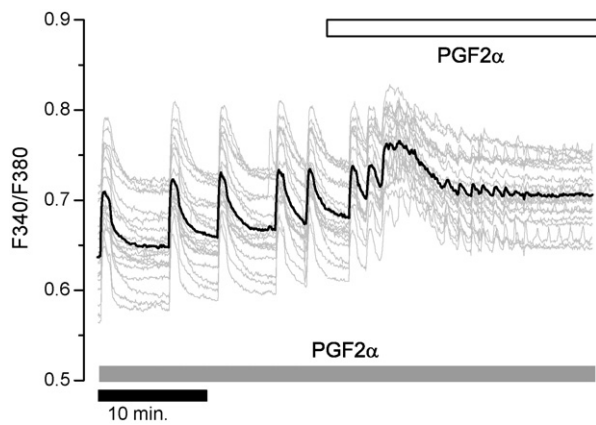


Figure 2 Synchrony of $\text{Ca}^{2+}/\text{Sr}^{2+}$ -transients measured outside the ring, induced by addition of $\text{PGF}_{2\alpha}$ ($0.5 \mu\text{M}$) inside the ring, is lost upon perfusion outside the ring with $0.5 \mu\text{M}$ $\text{PGF}_{2\alpha}$. A typical response of 20 cells is displayed ($n=5$ experiments). Individual traces are in gray, while the mean response is shown in black. Lower gray bar indicates presence of $\text{PGF}_{2\alpha}$ inside the ring, top hollow bar indicates perfusion with $\text{PGF}_{2\alpha}$ outside the ring. Time (10 min) is indicated by the lower black bar.

Pacemaking activity requires a transitional zone between $\text{PGF}_{2\alpha}$ -treated and non-treated cells

We have previously shown that IP_3 -mediated calcium oscillations in $\text{PGF}_{2\alpha}$ -treated NRK cells occur asynchronously, in spite of electrical coupling between the cells [14]. In contrast, in the ring experiments propagating calcium action potentials outside the ring persisted, causing almost synchronous calcium transients in the follower cells. In order to investigate the requirement of a transient tissue zone between the $\text{PGF}_{2\alpha}$ -treated cells in the ring and the untreated cells outside the ring, we first measured calcium oscillations outside the ring after the addition of $0.5 \mu\text{M}$ $\text{PGF}_{2\alpha}$ inside the ring. Fig. 2 shows that $\text{PGF}_{2\alpha}$ addition inside the ring resulted in synchronous high amplitude, low frequency calcium transients outside the ring, most likely as a consequence of the periodic passage of action potentials. Subsequently the same cells outside the ring were analyzed upon addition of $0.5 \mu\text{M}$ $\text{PGF}_{2\alpha}$ to the perfusion medium, thereby annihilating the $\text{PGF}_{2\alpha}$ -gradient across the ring. Fig. 2 shows that under these conditions asynchronous low amplitude, high frequency calcium oscillations were observed ($n=5$), which are characteristic for $\text{PGF}_{2\alpha}$ -treated cells [14]. These data show that in follower cells the apparent synchronization of calcium oscillations, due to propagation of action potentials, is rapidly lost upon treatment with $\text{PGF}_{2\alpha}$. This is most likely due to annihilation of the pacemaker mechanism in the transient tissue zone under the ring as a consequence of the inactivation of the L-type calcium channels, which results from sustained depolarization of the cells following to activation of calcium-activated chloride channels [7]. Comparable results ($n=4$) were obtained in patch-clamp recordings. Subsequent perfusion with $\text{PGF}_{2\alpha}$ outside the ring resulted in a depolarization to approximately -20mV causing annihilation of the periodic action potentials (data not shown). We conclude that in this experimental set-up, an intercellular

$[\text{IP}_3]$ -gradient is achieved, by adding a hormone locally in the ring, that provides an area of cells with the 'proper' $[\text{IP}_3]$ required for induction of pacemaking activity. Whether the intercellular gradient of IP_3 originates from a gap junctional diffusion of IP_3 from cells inside the ring to those under and outside the ring, or whether extracellular $\text{PGF}_{2\alpha}$ under the ring contributes to this IP_3 -gradient remains to be established.

Synchronization of Ca^{2+} -oscillations occurs under the ring

The above results indicate that $\text{PGF}_{2\alpha}$ -treated cells inside the ring are essential for the generation of periodic calcium action potentials outside the ring, but these experiments do not provide information about the location of pacemaker areas. To form a pacemaker area that is able to initiate action potentials cells have to synchronize their IP_3 -mediated calcium oscillations. Fig. 3 compares the extent of synchronization of intracellular calcium oscillations outside, inside and under the ring, following addition of $\text{PGF}_{2\alpha}$ inside the ring. The data show that the near-synchronous individual calcium transients recorded outside the ring had dominant interval times of 4.0 and 4.3 min ($n=123$) in the experiment presented in Fig. 3A (right panel), while inside the ring asynchronous oscillations with a broad range of frequencies were observed (median interval time 1.3 min, $n=376$). Inside the ring (Fig. 3C) 90% of the asynchronous oscillations had an interval time between 0.5 and 2.8 min (Fig. 3C). Under the ring, however, a more dominant pattern of synchronous oscillations was observed (Fig. 3B) whereby 90% of the oscillations had an interval time between 1.0 and 2.3 min (median interval time 1.5 min, $n=246$).

Averaged over seven experiments, we observed a value of 2.0 ± 0.5 min (mean \pm S.D.) for the most dominant interval time between calcium oscillations under the ring, while in the same experiments a value of 3.9 ± 1.3 min was observed for the interval between calcium transients outside the ring. When these values were compared pairwise for the same experiment a ratio of 2.0 ± 0.6 ($n=7$) was observed for the interval time outside and under the ring. However, in individual experiments ratios of 1.0 and 3.0 were observed as well. The observation that the interval time between calcium transients under the ring is shorter than outside the ring, suggests that calcium oscillations under the ring may induce action potentials outside the ring with a particular entrainment.

Simulation of calcium action potentials in a two-dimensional network

To explore the experimental findings for quiescent NRK cell monolayers in which periodic calcium action potentials are induced outside the ring by application of $\text{PGF}_{2\alpha}$ to the cells inside the ring, we carried out numerical computer simulations in the model described in Materials and methods. The $\text{PGF}_{2\alpha}$ enhanced intracellular IP_3 concentration in cells within the ring has two effects, a direct and an indirect one. First it gives rise to an increase of the intracellular calcium concentration, which by activation of calcium-activated chloride-channels depolarizes the cells.

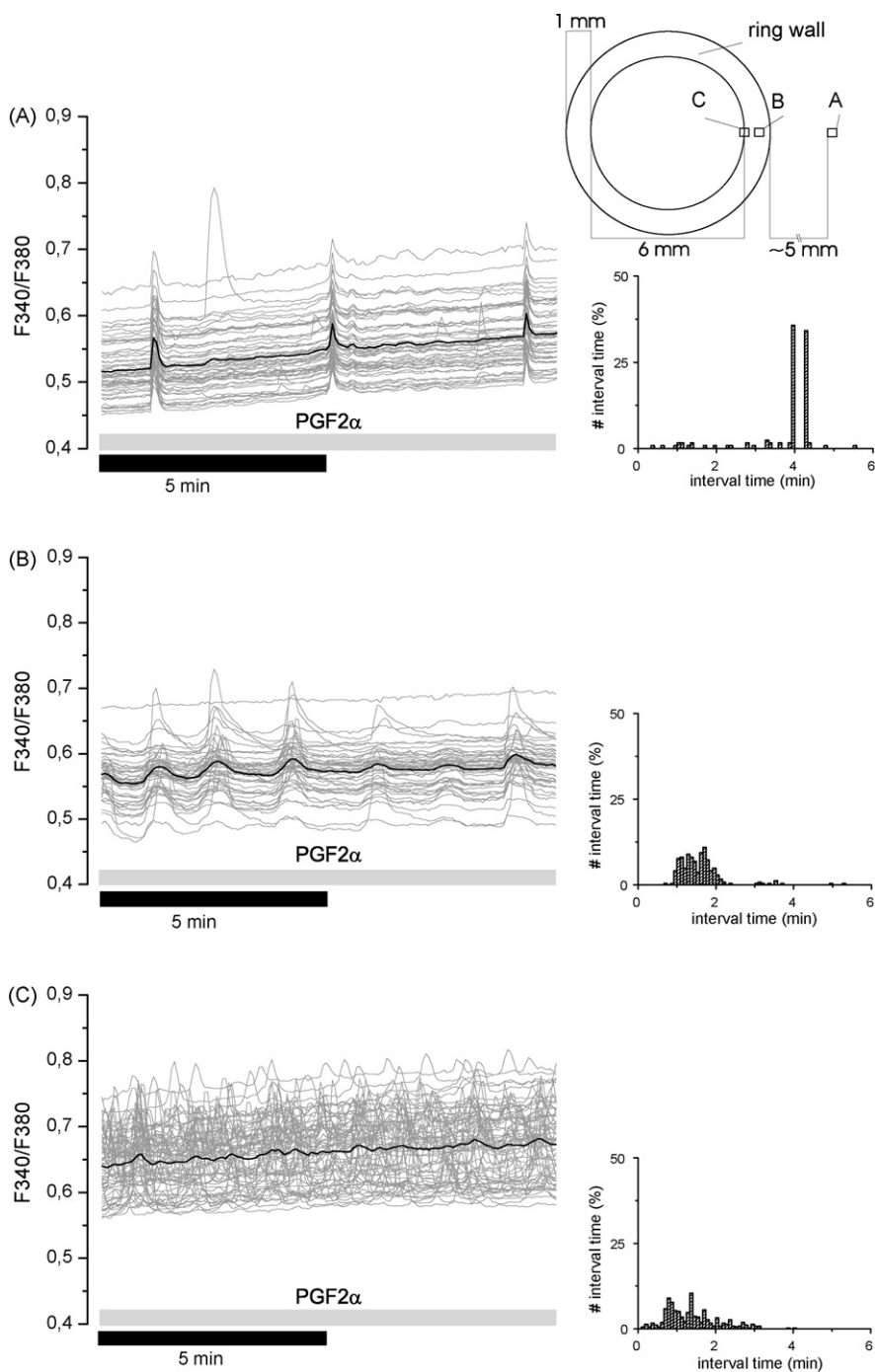


Figure 3 Changes in intracellular $\text{Ca}^{2+}/\text{Sr}^{2+}$ levels of quiescent monolayer NRK cells, upon stimulation with $\text{PGF}_{2\alpha}$ inside the ring, at different positions outside, inside and under the ring. Cells inside the ring were stimulation with $\text{PGF}_{2\alpha}$ ($n=7$ experiments). Distribution of the interval time between calcium oscillations is depicted at right panels. (A) Response of 62 cells measured 5 mm outside the ring at position A (see inset) after addition inside the ring of $0.8 \mu\text{M}$ $\text{PGF}_{2\alpha}$. (B) Response of 47 cells measured under the ring (position B in inset) in the presence of $\text{PGF}_{2\alpha}$ inside the ring. (C) Response of 67 cells measured at the inner edge of the ring (position C in inset) in the presence of $\text{PGF}_{2\alpha}$ inside the ring. Individual traces are shown in gray, the mean response of the imaged cells is represented by the black line. Cells outside the ring were perfused with 5 mM Sr^{2+} , while inside the ring 1 mM Ca^{2+} was present (see Materials and methods). The lower gray bar indicates presence of $\text{PGF}_{2\alpha}$ inside the ring. Inset shows different positions of the imaged regions in relation to the ring location on the monolayer. Time (5 min) is indicated by the lower black bar.

Secondly, locally produced IP_3 will diffuse to adjacent cells via gap junctions.

In general there are two classes of models by which IP_3 may cause oscillations in intracellular calcium concentration [23]. Ca^{2+} -oscillations may either be caused by sequential positive and negative feedback of Ca^{2+} on the IP_3 -receptor and occur at constant (steady-state) $[\text{IP}_3]$, or be directly dependent on oscillations in $[\text{IP}_3]$. In the first case the frequency of the calcium oscillation is an increasing function of $[\text{IP}_3]$. If in such a case a pulse of IP_3 is applied to a cell exhibiting Ca^{2+} -oscillations, the additional IP_3 will cause a transient increase in the oscillation frequency, as pointed out by Sneyd et al. [24]. Conversely, for cells in which the calcium oscillations depend on $[\text{IP}_3]$ and thus can occur only when $[\text{IP}_3]$ is in the appropriate range, the application of an external pulse of IP_3 will force $[\text{IP}_3]$ out of this oscillatory range, and the oscillations cannot reappear until $[\text{IP}_3]$ has decreased sufficiently, thus causing a change in the phase of the oscillations. The assumption that in NRK fibroblasts IP_3 -dependent calcium oscillations arise from the kinetics of the IP_3 -receptor and thus depend on the steady-state IP_3 -concentration, is supported by results of an experiment performed in conformity with Sneyd et al. [24] (see Supplemental file II). Therefore in the model we assumed a steady-state concentration of IP_3 in all cells depending on their respective position in the network (see Fig. 4A and Appendix A). This IP_3 concentration was set at a high value (average $10 \mu\text{M}$) for cells within the ring, and at a low value for cells far outside the ring ($0.1 \mu\text{M}$). In between, the concentration of IP_3 decreased according to a modified Bessel function (Fig. 4A, see also Appendix A), which describes the decay of the IP_3 concentration outside the ring due to diffusion of IP_3 through gap junctions.

Quiescent NRK cells far outside the ring have a membrane potential of -70 mV , while cells treated with $0.5 \mu\text{M}$ $\text{PGF}_{2\alpha}$ in the middle of the ring are depolarized to -20 mV as a result of the sustained opening of calcium-activated chloride-channels [6]. Fig. 4B (solid line) shows the profile of the simulated voltage gradient across the ring, for gap junction conductance of 3 nS . Due to the membrane potential difference between the cells in the ring and those under the ring, there will result a constant current through the gap junctions, which explains why cells inside, but near the edge of the ring show a membrane potential that is below -20 mV (Fig. 4B, position C). The profile of this voltage gradient will be strongly affected, however, by diffusion of IP_3 , which shows the concentration profile in Fig. 4A. The increased IP_3 concentration for cells under the ring ($r > 1 \text{ mm}$) leads to an increase in the intracellular calcium concentration and a concomitant depolarization (dashed line in Fig. 4B).

Fig. 5 shows the results of simulations of the intracellular calcium concentration (left column) and membrane potential (right column) for a cluster of cells outside (panel A), under (panels B1 and B2) and inside/under the ring (panel C). These panel numbers correspond to different locations relative to the ring, as shown in the inset of Fig. 4. At each position, the activity of a cluster of 25 cells is shown, corresponding to an area of $50 \mu\text{m} \times 50 \mu\text{m}$. The cells inside and just under the ring (position C) have a relatively high IP_3 concentration in a range between 5 and $15 \mu\text{M}$, characteristic for $\text{PGF}_{2\alpha}$ -treated cells. For IP_3 -concentrations

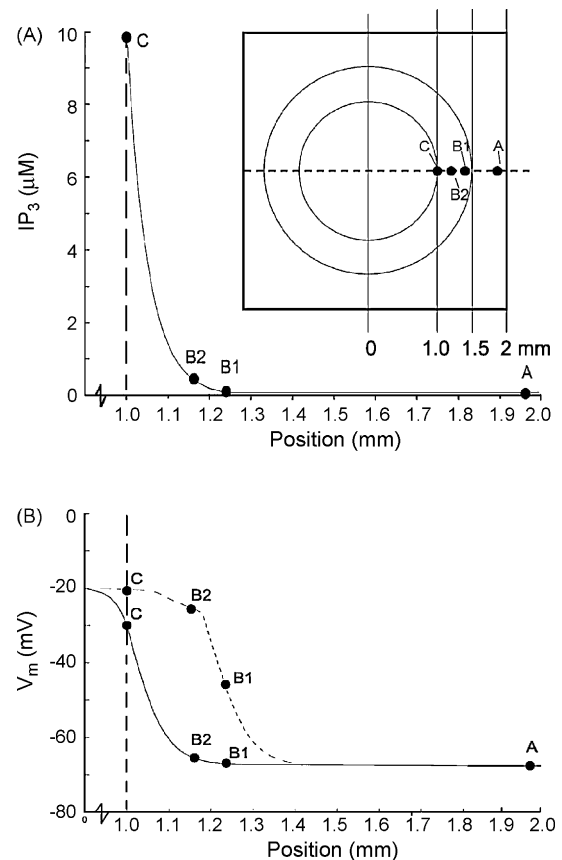


Figure 4 The inset shows a schematic two-dimensional network of 400×400 cells. At the centre of the network, within a ring with an inner radius of 1 mm (equivalent to 100 cells) have an IP_3 concentration randomly distributed within a range between 5 and $15 \mu\text{M}$. (A) IP_3 gradient due to diffusion and degradation of IP_3 as described by Eq. (A.4) in Appendix A. For cells under the ring (0.5 mm thick) the IP_3 concentration decreases according to Eq. (A.4) from $10 \mu\text{M}$ (inner side of the ring) to $0.1 \mu\text{M}$ (outside the ring). Cells outside the ring have an IP_3 -concentration of $0.1 \mu\text{M}$ and do not exhibit spontaneous calcium oscillations. (B) Membrane potential gradient in the network with (dashed line) and without (solid line) taking into account IP_3 diffusion. The solid line shows the average membrane potential if there would be no diffusion of IP_3 from the inside of the ring to cells under the ring. The dashed line shows the average membrane potential as a result of simulations for an IP_3 distribution in the network according to Eq. (A.4) in Appendix A.

between 5 and $8.5 \mu\text{M}$, this will trigger periodic calcium release from IP_3 -sensitive ER stores, resulting in uncorrelated and asynchronous calcium oscillations. For cells with an IP_3 concentration between 8.5 and $15 \mu\text{M}$, the IP_3 receptor leaks calcium ions continuously from intracellular calcium stores, causing an elevated calcium concentration in the cells without oscillations. The left panel of Fig. 5C shows a superposition of the calcium traces for the various cells. Some cells show more or less periodic calcium oscillations, whereas other cells reveal a constant, elevated calcium concentration. The right panel of Fig. 5C shows that the elevated intracellular calcium concentration of these

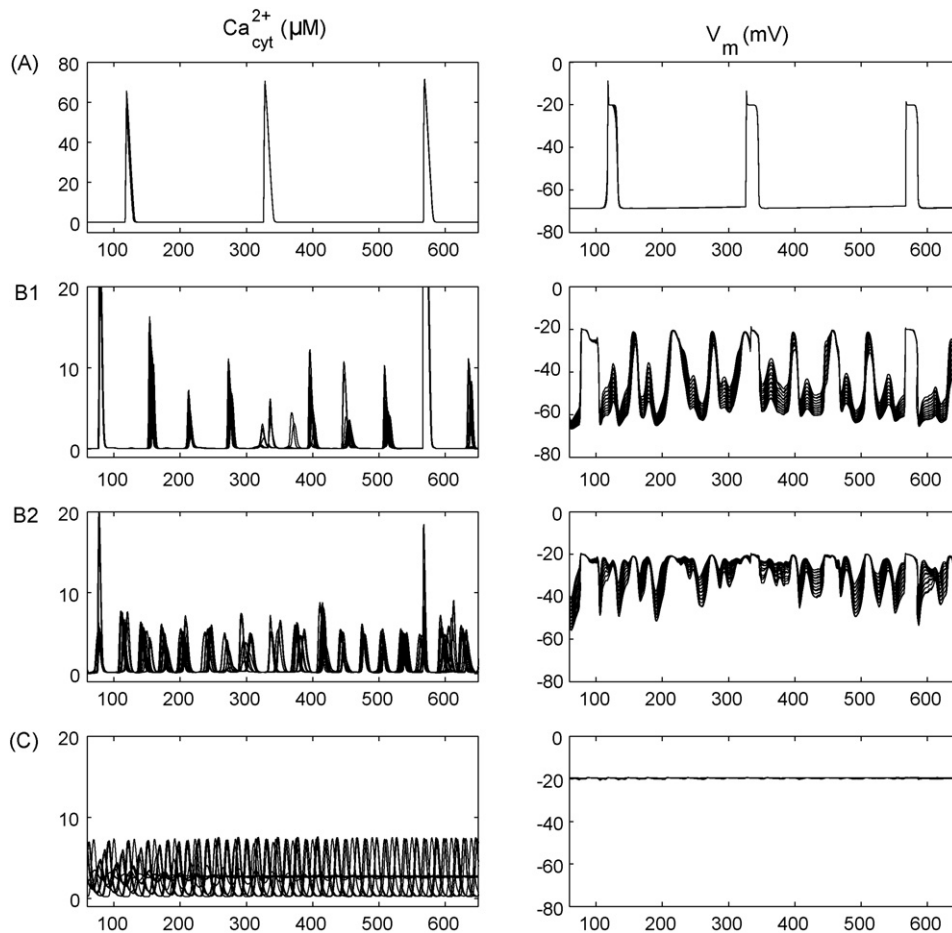


Figure 5 The membrane potential (right column) and corresponding intracellular calcium concentrations (left column) of our simulation study for the 2D-network for cells outside (panel A), under the ring (panels B1 and B2) and inside/under the ring (panel C) (respectively 1.97, 1.24, 1.16 mm and 1.0 mm from the centre of the ring), corresponding to the positions A, B1, B2 and C in the inset of Fig. 4. Each panel shows a superposition of 25 traces of the 25 cells in the $50 \mu m \times 50 \mu m$ area at A, B1, B2 and C.

cells causes a depolarization to about -20 mV. Since all cells inside the ring have a similar membrane potential near -20 mV, the current through the gap junctions is negligible.

In cells under the ring along the steady-state gradient of intracellular IP_3 , the 25 cells near position B2 have an IP_3 concentration between approximately 0.3 and $0.8 \mu M$, while for cells near position B1 this ranges from 0.15 and $0.25 \mu M$ (see Fig. 4A). In isolated cells, IP_3 concentrations in that range will induce intracellular calcium oscillations by release of calcium from IP_3 -sensitive ER stores. At position B2 the membrane potential fluctuates around -25 mV (see Fig. 4B), which will keep the L-type calcium channel mostly in an inactive form. However, due to fluctuations in the membrane potential these cells occasionally repolarize to values below -40 mV and during subsequent depolarization the L-type calcium channels may transiently open. As a consequence the calcium oscillations in these cells tend to synchronize (see Fig. 5B2), in spite of the fact that most of the time the L-type calcium channels remain closed. As explained by Timme et al. [25] weak coupling between oscillators with different frequencies or weak noise in identical, synchronized oscillators can cause perpetual

synchronization and desynchronization with continuously varying clusters.

At position B1 the membrane potential constantly varies between -60 and -20 mV. Highly synchronized changes in intracellular calcium concentration take place, which coincide with the depolarization phase (see Fig. 5B1). The intracellular calcium concentration rises to higher levels than in cells at position B2. This can be understood by a substantial contribution of a calcium influx via activated L-type calcium channels, which are more inactivated at B2 than at position B1. These data agree with previous modeling results which show that at membrane potentials below the window current of the L-type calcium channel near -35 mV, rapid depolarization of the cells by calcium transients can provide effective coupling of calcium oscillations [20]. The observation that cells at B1 show highly synchronized calcium oscillations, in combination with opening of the L-type calcium channels, makes them ideal candidates to act as the pacemaker cells to generate propagating calcium action potentials in the follower cells.

Cells at position A behave as follower cells and transmit the received action potentials (right panel, Fig. 5A) to

their neighbors resulting in calcium oscillations simultaneously with the action potentials (see left panel, Fig. 5A). Intriguingly, the frequency of the calcium oscillations for the cells at A is much lower than at B1. Approximately one out of four calcium oscillations at B1 corresponds to a calcium transient in the cells at A. This lower frequency can be understood when taking into account the activation and inactivation kinetics of the IP₃ receptor. In our model, the IP₃ receptor inactivates at elevated calcium concentrations and de-inactivates when the cytoplasmic calcium concentration decreases. The speed of both processes is increased at elevated IP₃ concentrations [19–21]. This indicates that for low IP₃ concentrations (near 0.1 μM as in follower cells) the time constant for de-inactivation of the IP₃ receptor is long (in the order of 200 s), while for the higher IP₃ concentrations near positions B1 and B2, this time constant is about 50–100 s. Since the time constant in the follower cells is long (about 200 s) relative to the time interval between action potentials generated by the pacemaker cell (about 50–100 s), the de-inactivation of the IP₃ receptor in the follower cells has not yet recovered after a depolarization to –20 mV in the pacemaker cells. Therefore, the IP₃ receptor channels of these cells cannot be sufficiently activated when the pacemaker area generates the next action potential. As a result, the frequencies of calcium oscillations in follower cells tend to be lower than those of pacemaker cells but entrained with pacemaker firing.

Discussion

Density-arrested NRK fibroblasts show spontaneous calcium action potentials which propagate through the cellular monolayer. Using a new experimental set-up in which a ring was placed on top of the monolayer, we now show that local application of PGF_{2α} to quiescent NRK cells is sufficient to induce formation of the pacemaker cells that are required for the generation of such action potentials.

We have previously postulated that density-arrested NRK monolayers contain groups of cells which produce enhanced amounts of PGF_{2α} and thereby act as local pacemaker centers for the observed action potentials, while the remaining cells act as followers which participate in the propagation of these action potentials. However, such pacemaker centers have not been identified by specific markers and may even have a transient character. As a consequence it has not been possible so far to study the properties of such pacemaker cells in NRK monolayers. Previously we have shown that activators of Gq-coupled protein receptors can induce changes in the membrane potential and IP₃-mediated calcium oscillations within their target cells [14]. Using the current ring approach, which allowed us to separate pacemaker and follower cells, we now show that as a result of electrical coupling and diffusion of IP₃ through the gap junctions between treated and non-treated cells, cells under the ring have the proper membrane potential and IP₃-mediated calcium oscillations to form a pacemaker area for the generation of calcium action potentials. These data imply that the formation of pacemaker areas in cellular monolayers requires a combination of coupled PGF_{2α}-stimulated and non-stimulated cells. The stimulated cells supply the required IP₃ for calcium oscil-

lations, while the non-stimulated cells provide the required membrane potential for opening of the L-type calcium channel.

In other systems where calcium action potentials have been studied, pacemaker and follower cells are distinct cell types. Also in those systems pacemaking activity requires an initial depolarization process followed by activation of voltage-dependent calcium channels. In sinoatrial node intracellular calcium oscillations in the pacemaker cells activate Na⁺–Ca²⁺-exchange, which results in sodium influx and subsequent depolarization [26], while in smooth muscle cells activation of a calcium-activated chloride current mediates cell depolarization [27,28].

PGF_{2α} is known to induce asynchronous calcium oscillations in quiescent NRK cells, in spite of a substantial gap junctional coupling of the cells [14]. It should be noted that this unsynchronized behaviour of the cells upon exposure to a high concentration of PGF_{2α} cannot be attributed to a loss of gap junctional coupling of the cells. Previously we have shown that addition of a high concentration of PGF_{2α} to a quiescent monolayer of NRK cells, resulting in an increased cytosolic calcium concentration, did not affect the gap junctional coupling between the cells [14].

Although we cannot exclude the occurrence of [IP₃]-oscillations in NRK-fibroblasts after receptor activation, there are no indications that the PGF_{2α}-induced calcium oscillations in these cells depend on [IP₃]-oscillations. These asynchronous calcium oscillations indicate that Ca²⁺ diffusion through gap junctions is not very effective in these cells. Moreover, electrical coupling is far more efficient than chemical coupling by diffusion of Ca²⁺ [20,29]. Diffusion through gap junctions does play a role, however, in that it enables IP₃ to establish a steady state gradient of excitability rather than a direct beat-to-beat coupling of oscillators. A plausible explanation for the synchronization of calcium oscillations between cells in pacemaking areas is that it occurs by electrical signal transmission through the gap junctions. The calcium waves evoked depolarizations or action potentials (Fig. 5B1) via calcium-activated chloride-channels. Then the depolarizations or action potentials are conducted to neighbor cells and cause calcium inflow through the L-type channels in these cells to activate the IP₃-receptors and in this way to synchronize the calcium waves. This is shown experimentally in Fig. 2 where the synchronicity of the cells, observed during propagation of calcium action potentials, is rapidly lost upon addition of PGF_{2α}. Both the experimental data (Fig. 3) and theoretical analysis (Fig. 5) shows that the calcium oscillations gradually synchronize when moving from positions inside to those under the ring. Our data are in line with recent results of Kusters et al. [19,20] and those of other groups [30–32] who have studied how IP₃-mediated Ca²⁺-oscillations can be involved in the generation of cellular pacemaking activity.

In the present experiments, extracellular calcium outside the ring was replaced by strontium which ensures a more robust propagation of action potentials [5]. Under conditions of extracellular strontium instead of calcium the conductance of L-type calcium channels becomes higher, while ion-dependent inactivation of this conductance is lower [7]. Therefore in our model equations we have neglected the calcium-dependent inactivation factor for the L-type calcium channel and increased the L-type calcium channel

conductance [20]. The replacement of calcium by strontium thus ensures a more pronounced depolarization of the cells upon opening of the L-type calcium channels, which may facilitate the generation of action potentials in the follower cells. Inside the ring extracellular calcium was not replaced by strontium since in PGF_{2α}-treated cells the L-type calcium channels are already inactivated as a result of the depolarization, while extracellular calcium enables a more sensitive identification of the calcium oscillations inside and under the ring than strontium. Density-arrested NRK cells show spontaneous action potentials in strontium-containing medium, indicating that strontium does not interfere with the pacemaking activity of NRK cells [6,14].

Interestingly, the average interval time between calcium action potentials measured outside the ring was almost twice the average interval time between calcium oscillations under the ring. This suggests an 1:2 entrainment in the follower cells (Fig. 3), although incidentally 1:1 entrainment has been observed as well in our study (data not shown). In comparison with the simulation studies, where we explained an 1:4 entrainment (Figs. 5A and 5B1) by the refractory period of the IP₃ receptor, simulations with a somewhat higher IP₃ concentration would have enabled 1:2 entrainment. This can occur under conditions of a slightly higher IP₃ concentration in the follower cells, as a consequence of either a more favorable ratio between degradation (λ) and diffusion (D_{IP_3}) or a somewhat higher IP₃-receptor sensitivity or production of IP₃. Different modes of entrainment have been described for an one-dimensional model of NRK fibroblast by Kusters et al. [20]. Entrainment in smooth muscle cells and cardiac cells has been described earlier as the Wenckebach phenomenon [33].

The pacemaker mechanism created in ring experiments on quiescent NRK cell cultures may be similar to the one we have described in density-arrested cultures. Therefore, we hypothesize for those cultures the existence of inhomogeneity in the local production of PGF_{2α} which can give rise to islands of depolarized cells with increased intracellular IP₃. Gap junctional coupling between the cells would then allow the establishment of a membrane potential gradient and IP₃ concentration gradient towards the surrounding cells with a more negative membrane potential and a lower IP₃ concentration. A transitional pacemaker area driving the surrounding follower cells would then arise as observed in the ring experiments on quiescent cells. It should be noted that a gradient of IP₃-concentration per se is not essential for establishing a pacemaker zone, but that rather achieving the 'proper' intracellular IP₃ concentration allows a group of cells to exhibit pacemaking activity (see Supplemental file III). However, in our mathematical modelling we assumed an [IP₃]-gradient since this would be more analogous to conditions in our experimental set-up. Moreover, we hypothesize that this set-up would also be more analogous to conditions in pacemaker areas in density arrested cultures of NRK fibroblasts, since it seems likely that the cells in such cultures will differ substantially in their [IP₃]. Mapping action potential firing with a multi-electrode system would be a necessary experiment to evaluate this pacemaker hypothesis for density-arrested cells.

We conclude that the local application of an IP₃ producing hormone promotes a pacemaking and propagation mechanism that consists of the intricate cooperation of the

intracellular calcium handling-system and the voltage- and calcium-dependent properties of the ion channels in the plasma membrane. This mechanism seems to be of general importance for calcium signal transmission across various tissues as for example in vascular smooth muscles playing a role in vasomotion [34].

Conflict of interest

There is no conflict of interest in publishing the experimental results regarding this manuscript by any author for publication to Cell Calcium.

Acknowledgement

This research project was funded by The Netherlands Organization for Scientific Research (NWO; project 805.47.066).

Appendix A

In order to analyze theoretically the IP₃ concentration in a network of NRK cells, we assume that IP₃ is constitutively produced in cells within the ring as a result of PGF_{2α} treatment, giving rise to a mean intracellular concentration of 10 μM. Outside the ring, the intracellular IP₃ concentration depends on diffusion from the cells in the ring to the other cells in the network, in combination with degradation of IP₃.

Assuming that the cells under and outside the ring do not produce IP₃, the concentration gradient of IP₃ as a function of position (\vec{x}) and time (t) due to degradation and diffusion is given by the general diffusion equation

$$\frac{\delta IP_3}{\delta t} = D_{IP_3} \nabla^2 IP_3(\vec{x}, t) - \lambda IP_3(\vec{x}, t) \quad (A.1)$$

where D_{IP_3} is the diffusion coefficient of IP₃ and λ is the rate of IP₃ degradation. To solve the two-dimensional diffusion equation we change from Cartesian coordinates \vec{x} to polar coordinates (r and ϕ), which results in:

$$\frac{\delta IP_3(r, \phi)}{\delta t} = D_{IP_3(r, \phi)} \left[\frac{\partial^2}{\partial r^2} IP_3(r, \phi) + \frac{1}{r} \frac{\partial}{\partial r} IP_3(r, \phi) + \frac{1}{r^2} \frac{\partial^2}{\partial \phi^2} IP_3(r, \phi) \right] - \lambda IP_3(r, \phi) \quad (A.2)$$

For reasons of circular symmetry, the term $(1/r^2)(\partial^2/\partial \phi^2)IP_3(r, \phi)$ is zero. For a constant concentration of IP₃ in the pacemaker cluster, the steady-state solution to Eq. (A.1) should obey

$$\frac{\delta^2}{\delta r^2} IP_3 + \frac{1}{r} \frac{\delta}{\delta r} IP_3 - \frac{\lambda}{D_{IP_3}} IP_3 = 0 \quad (A.3)$$

The solution to this equation is the modified Bessel-function of order zero [35]. The boundary condition that the solution should be finite for $r \uparrow \infty$ leads to the solution which for sufficiently large values of r is given by

$$IP_3(r) = B \left(\frac{\pi}{2rp} \right)^{1/2} e^{-rp} + \text{constant} \quad (A.4)$$

with

$$\rho = \sqrt{\frac{\lambda}{D_{IP_3}}}$$

The following values for the diffusion coefficient D_{IP_3} and for λ were taken from the literature (see [36–38]: $D_{IP_3} = 258 \mu\text{m}^2 \text{s}^{-1}$ and $\lambda = 0.07 \text{s}^{-1}$). With these values $\rho \approx 0.0165 \mu\text{m}^{-1}$. With the boundary conditions that the concentration of IP_3 has a mean value of $10 \mu\text{M}$ inside the ring ($0 \leq r \leq 1 \text{mm}$), and a value of $0.1 \mu\text{M}$ at large distances from the ring we find

$$IP_3(r) = 10 \mu\text{M}, \quad \text{for } 0 \leq r \leq 1 \text{mm}$$

$$IP_3(r) = B \left(\frac{\pi}{2\rho r} \right)^{1/2} e^{-\rho r} + 0.1 \mu\text{M}, \quad \text{for } r \geq 1 \text{mm}$$

where the value of B is such that $IP_3(r)$ is a continuous function with $IP_3(1 \text{mm}) = 10 \mu\text{M}$.

Appendix B. Supplementary data

Supplementary data associated with this article can be found, in the online version, at [doi:10.1016/j.ceca.2008.02.005](https://doi.org/10.1016/j.ceca.2008.02.005).

References

- [1] N. McHale, M. Hollywood, G. Sergeant, K. Thornbury, Origin of spontaneous rhythmicity in smooth muscle, *J. Physiol.* 570 (2006) 23–28.
- [2] S.S. Stojilkovic, H. Zemkova, F. Van Goor, Biophysical basis of pituitary cell type-specific Ca^{2+} signaling-secretion coupling, *Trends Endocrinol. Metab.: TEM* 16 (2005) 152–159.
- [3] J.M. Ramirez, A.K. Tryba, F. Pena, Pacemaker neurons and neuronal networks: an integrative view, *Curr. Opin. Neurobiol.* 14 (2004) 665–674.
- [4] A. De Roos, P.H. Willems, E.J. van Zoelen, A.P. Theuvenet, Synchronized Ca^{2+} signaling by intercellular propagation of Ca^{2+} action potentials in NRK fibroblasts, *Am. J. Physiol.* 273 (1997) C1900–C1907.
- [5] A.D. de Roos, P.H. Willems, P.H. Peters, E.J. van Zoelen, A.P. Theuvenet, Synchronized calcium spiking resulting from spontaneous calcium action potentials in monolayers of NRK fibroblasts, *Cell Calcium* 22 (1997) 195–207.
- [6] E.G. Harks, P.H. Peters, J.L. van Dongen, E.J. van Zoelen, A.P. Theuvenet, Autocrine production of prostaglandin F2alpha enhances phenotypic transformation of normal rat kidney fibroblasts, *Am. J. Physiol. Cell Physiol.* 289 (2005) C130–C137.
- [7] E.G. Harks, J.J. Torres, L.N. Cornelisse, D.L. Ypey, A.P. Theuvenet, Ionic basis for excitability of normal rat kidney (NRK) fibroblasts, *J. Cell Physiol.* 196 (2003) 493–503.
- [8] R.J. Lang, M.F. Klemm, Interstitial cell of Cajal-like cells in the upper urinary tract, *J. Cell. Mol. Med.* 9 (2005) 543–556.
- [9] K.J. Park, G.W. Hennig, H.T. Lee, N.J. Spencer, S.M. Ward, T.K. Smith, K.M. Sanders, Spatial and temporal mapping of pacemaker activity in interstitial cells of Cajal in mouse ileum in situ, *Am. J. Physiol. Cell Physiol.* 290 (2006) C1411–C1427.
- [10] K.M. Sanders, S.D. Koh, S.M. Ward, Interstitial cells of Cajal as pacemakers in the gastrointestinal tract, *Ann. Rev. Physiol.* 68 (2006) 307–343.
- [11] G.P. Sergeant, M.A. Hollywood, N.G. McHale, K.D. Thornbury, Ca^{2+} signalling in urethral interstitial cells of Cajal, *J. Physiol.* 576 (2006) 715–720.
- [12] A. Shafik, A.A. Shafik, O. El Sibai, I.A. Shafik, Specialized pacemaking cells in the human Fallopian tube, *Mol. Hum. Reprod.* 11 (2005) 503–505.
- [13] V. Pucovsky, M.I. Harhun, O.V. Povstyan, D.V. Gordienko, R.F. Moss, T.B. Bolton, Close relation of arterial ICC-like cells to the contractile phenotype of vascular smooth muscle cell, *J. Cell. Mol. Med.* 11 (2007) 764–775.
- [14] E.G. Harks, W.J. Scheenen, P.H. Peters, E.J. van Zoelen, A.P. Theuvenet, Prostaglandin F2 alpha induces unsynchronized intracellular calcium oscillations in monolayers of gap junctionally coupled NRK fibroblasts, *Pflugers Arch.* 447 (2003) 78–86.
- [15] T. Hofer, A. Politi, R. Heinrich, Intercellular Ca^{2+} wave propagation through gap-junctional Ca^{2+} diffusion: a theoretical study, *Biophys. J.* 80 (2001) 75–87.
- [16] T. Tordjmann, B. Berthon, M. Claret, L. Combettes, Coordinated intercellular calcium waves induced by noradrenaline in rat hepatocytes: dual control by gap junction permeability and agonist, *EMBO J.* 16 (1997) 5398–5407.
- [17] L.N. Cornelisse, R. Deumens, J.J. Coenen, E.W. Roubos, C.C. Gielen, D.L. Ypey, B.G. Jenks, W.J. Scheenen, Sauvagine regulates Ca^{2+} oscillations and electrical membrane activity of melanotrope cells of *Xenopus laevis*, *J. Neuroendocrinol.* 14 (2002) 778–787.
- [18] J.M. Kusters, J.M. Cortes, W.P. van Meerwijk, D.L. Ypey, A.P. Theuvenet, C.C. Gielen, Hysteresis and bistability in a realistic cell model for calcium oscillations and action potential firing, *Phys. Rev. Lett.* 98 (2007) 098107.
- [19] J.M. Kusters, M.M. Dernison, W.P. van Meerwijk, D.L. Ypey, A.P. Theuvenet, C.C. Gielen, Stabilizing role of calcium store-dependent plasma membrane calcium channels in action-potential firing and intracellular calcium oscillations, *Biophys. J.* 89 (2005) 3741–3756.
- [20] J.M. Kusters, W.P. van Meerwijk, D.L. Ypey, A.P. Theuvenet, C.C. Gielen, Fast calcium wave propagation mediated by electrically conducted excitation and boosted by CICR, *Am. J. Physiol.*, in press.
- [21] J.K. Foskett, C. White, K.H. Cheung, D.O. Mak, Inositol trisphosphate receptor Ca^{2+} release channels, *Physiol. Rev.* 87 (2007) 593–658.
- [22] M. de Leon, Y. Wang, L. Jones, E. Perez-Reyes, X. Wei, T.W. Soong, T.P. Snutch, D.T. Yue, Essential $Ca(2+)$ -binding motif for $Ca(2+)$ -sensitive inactivation of L-type Ca^{2+} channels, *Science* 270 (1995) 1502–1506.
- [23] M.J. Berridge, A. Galione, Cytosolic calcium oscillators, *FASEB J.* 2 (1988) 3074–3082.
- [24] J. Sneyd, K. Tsaneva-Atanasova, V. Reznikov, Y. Bai, M.J. Sanderson, D.I. Yule, A method for determining the dependence of calcium oscillations on inositol trisphosphate oscillations, *Proc. Natl. Acad. Sci. U.S.A.* 103 (2006) 1675–1680.
- [25] M. Timme, F. Wolf, T. Geisel, Unstable attractors induce perpetual synchronization and desynchronization, *Chaos* 13 (2003) 377–387.
- [26] V.A. Maltsev, T.M. Vinogradova, E.G. Lakatta, The emergence of a general theory of the initiation and strength of the heartbeat, *J. Pharmacol. Sci.* 100 (2006) 338–369.
- [27] G.D. Hirst, N.J. Bramich, N. Teramoto, H. Suzuki, F.R. Edwards, Regenerative component of slow waves in the guinea-pig gastric antrum involves a delayed increase in $[Ca^{2+}]_i$ and $Cl(-)$ channels, *J. Physiol.* 540 (2002) 907–919.
- [28] Q. Wang, R.C. Hogg, W.A. Large, Properties of spontaneous inward currents recorded in smooth muscle cells isolated from the rabbit portal vein, *J. Physiol.* 451 (1992) 525–537.
- [29] D.F. van Helden, M.S. Imtiaz, Ca^{2+} phase waves: a basis for cellular pacemaking and long-range synchronicity in the guinea-pig gastric pylorus, *J. Physiol.* 548 (2003) 271–296.

- [30] H.M. Cousins, F.R. Edwards, H. Hickey, C.E. Hill, G.D. Hirst, Electrical coupling between the myenteric interstitial cells of Cajal and adjacent muscle layers in the guinea-pig gastric antrum, *J. Physiol.* 550 (2003) 829–844.
- [31] M.S. Imtiaz, C.P. Katnik, D.W. Smith, D.F. van Helden, Role of voltage-dependent modulation of store Ca^{2+} release in synchronization of Ca^{2+} oscillations, *Biophys. J.* 90 (2006) 1–23.
- [32] M.S. Imtiaz, J. Zhao, K. Hosaka, P.Y. von der Weid, M. Crowe, D.F. van Helden, Pacemaking through Ca^{2+} stores interacting as coupled oscillators via membrane depolarisation, *Biophys. J.* 92 (2007) 3843–3861.
- [33] R.M. Weiss, F.J. Tamarkin, M.A. Wheeler, Pacemaker activity in the upper urinary tract, *J. Smooth Muscle Res.* 42 (2006) 103–115.
- [34] C. Aelkjaer, H. Nilsson, Vasomotion: cellular background for the oscillator and for the synchronization of smooth muscle cells, *Br. J. Pharmacol.* 144 (2005) 605–616.
- [35] C.M. Bender, S.A. Orszag, *Advanced Mathematical Methods for Scientists and Engineers*, McGraw-Hill, Singapore, 1987.
- [36] N.L. Allbritton, T. Meyer, L. Stryer, Range of messenger action of calcium ion and inositol 1,4,5-trisphosphate, *Science* 258 (1992) 1812–1815.
- [37] G. Dupont, T. Tordjmann, C. Clair, S. Swillens, M. Claret, L. Combettes, Mechanism of receptor-oriented intercellular calcium wave propagation in hepatocytes, *FASEB J.* 14 (2000) 279–289.
- [38] J.D. Lechleiter, D.E. Clapham, Molecular mechanisms of intracellular calcium excitability in *X. laevis* oocytes, *Cell* 69 (1992) 283–294.